# Origin and Transformation of Ambient VOCs during a Dust-to-Haze Episode in Northwest China

Yonggang Xue[1,2,3,4], Yu Huang[1,2,3,4]*, Steven Sai Hang Ho[1,2,5], Long Chen[1,2,3,4], Liqin Wang[1,2,3,4], Shuncheng Lee[6], Junji Cao[1,2,3,4]*,

[1]Key Lab of Aerosol Chemistry & Physics, Institute of Earth Environment, Chinese Academy of Sciences, Xi'an 7 0061, China

[2]State Key Lab of Loess and Quaternary Geology (SKLLQG), Institute of Earth Environment, Chinese Academy of Sciences, Xi'an 710061, China

[3]Shaanxi Key Laboratory of Atmospheric and Haze-fog Pollution Prevention, Institute of Earth Environment, Chinese Academy of Sciences, Xi'an 710061, China

[4]CAS Center for Excellence in Quaternary Science and Global Change, Xi'an, 710061, China.

[5]Division of Atmospheric Sciences, Desert Research Institute, Reno, Nevada, USA

[6]Department of Civil and Environmental Engineering, The Hong Kong Polytechnic University, Hung Hom, Hong Kong, China

*Correspondence to*: Yu Huang (huangyu@ieecas.cn)

Junji Cao ( cao@loess.llqg.ac.cn)

**Abstract.** High contribution of secondary organic aerosol to the loading of fine particle pollution in China highlights the roles of volatile organic compounds oxidation. Therein, particulate active metallic oxides in dust, like $TiO_2$ and Fe ions, were proposed to influence the photochemical reactions of ambient VOCs. A case study was conducted at an urban site in Xi'an, northwestern China, to investigate the origin and transformation of VOCs during a windblown dust-to-haze pollution episode, and the assumption that dust would enhance the oxidation of VOCs was verified. Local vehicle exhaust (24.76%) and biomass burning (18.37%) were found to be the two largest contributors to ambient VOCs. In the dust pollution period, sharp decrease of VOCs loading and aging of their components were observed. Simultaneously, the secondary oxygenated VOCs fraction (i.e., methylglyoxal) increased. Source strength, physical dispersion, and regional transport were eliminated from the major factor for the variation of ambient VOCs. In another aspect, about 2 and 3 times increase of the loading of Iron (Fe) and titanium (Ti) was found in the airborne particle, together with fast decrease of trans-/cis-2-butene ratios which demonstrated that dust can accelerate the oxidation of ambient VOCs and formation of SOA precursors.

## 1 Introduction

Secondary aerosols are important components of fine particles in China, which could contribute to about 30 to 77 percent of $PM_{2.5}$ loading, therein, secondary organic aerosols (SOA) take about half of the loading (Huang et al., 2014). Guo et al. (2014) believed that gaseous emissions of volatile organic compounds (VOCs) and nitrogen oxides (NOx) were responsible for the large secondary PM formation. Laboratory experiments found OH-initiated oxidation of m-xylene could cause the coating thickness of black carbon, which further induced increase of particle size (1.5 to 10.4 times) and effective density (from 0.43 to 1.45 g $cm^{-3}$) (Guo et al., 2016).

Solid-gas heterogeneous reactions would cause the transformation of gaseous pollutants and change the property of particles (Zhang et al., 2000; Zhang et al., 2003; He et al., 2014). Recently, the oxidation of organic and inorganic gas on particles surface through the transitional-metal-catalyzed chain reaction was frequently found to play important roles on the transformation of ambient gas pollutants (Chu et al., 2019). Mineral dust is the most important sources of the transitional-metal, like Iron (Fe) and titanium (Ti), in the natural environment (Chen et al., 2012). In addition, mineral dust is one kind of the most abundant components of the global airborne PM, and about 1600 to 2000 Tg of mineral dust is transformed to aerosols annually from major deserts (Ginoux et al., 2001). Furthermore, the surface of mineral dust provides plenty of reactive sites for multiple atmospheric trace gas reactions (Cwiertny et al., 2008). As a result, dust was viewed to serve as catalyst for reactive gas, and modify the photochemical processes (Dentener et al., 1996; Dickerson et al., 1997).

With the controlled experiment of sulfate formation on mineral dust, Zhang et al. (2019) found that under appropriate humidity and particle acidity, surface transitional-metal-catalyzed chain reaction together with nitrate would highly accelerate the sulfate's formation on the surface of mineral dust (Zhang et al., 2019). In another aspect, gas-solid heterogeneous photochemical reactions of organic compounds were also reported on the illuminated surface of semiconductor metal oxides in the natural environment, in particular $TiO_2$ (Chen et al., 2012). Co-existence heterogeneous photochemical reactions of $SO_2$, $NO_2$ and VOCs on the surface of mineral dust were investigated in recent years. Both synergistic and suppress effects of VOCs on the formation of sulfate were found, which indicated the competition of reactive oxygen species and active sites between VOCs and inorganic gas pollutants (Chu et al., 2019; Song et al.,

60  2019). In addition, oxidized products, like formate and acetate species, were observed in the co-existence

61  reaction, which highlight the possibility of further oxidation of VOCs on the mineral dust (He et al., 2014).

62  In northwestern China, dust from both local sources and long-range transport is one of the most important

63  components of particulate matter of < 2.5 μm in diameter ($PM_{2.5}$) (Huang et al., 2014). Xi'an has a

64  population of ~8 million (Feng et al., 2016). The sharp increase of vehicles and other human activities has

65  led to high emissions of VOCs and $NO_x$ (Li et al., 2017). Observations showing simultaneous high dust

66  loading and elevated VOCs and $NO_x$ concentrations suggest possible impacts from heterogeneous reaction

67  on dust particles (Huang et al., 2014;Li et al., 2017). The present study was conducted to investigate the

68  origin and transformation of ambient VOCs with severe dust-to-haze episode in winter. The

69  transformation and the related chemical processing of ambient VOCs and the related changes in the

70  composition of $PM_{2.5}$ were studied, within typical windblown dust-to-haze episodes. The potential

71  pathway of VOCs oxidation in the windblown dust-to-haze formation process was explored.

72  **2 Materials and Methods**

73  **2.1 Sampling site**

74  An observation site (E 109°00′7", N 34°13′22") managed by Xi'an Jiaotong University was used in this

75  study (Figure 1). All sampling equipment was deployed on the rooftop of a 15-m tall academic building.

76  No obvious stationary pollution sources were found nearby, and the location can be considered as a typical

77  urban location in Xi'an (Zhang et al., 2015a).

78  **2.2 Field Sampling**

79  Severe dust-to-haze episode was observed in Xi'an and the surrounding areas from 8 November to 12

80  November in 2016, and samples was continuously collected during this period to investigate the chemical

81  compositions of both VOCs and fine PM. A total of 57 non-methane VOCs species (i.e., $C_2$-$C_{12}$ saturated

82  and unsaturated aliphatic and aromatic VOCs) were sampled hourly into offline multi-bed adsorbent tubes;

83  the measured 57 VOCs were defined as $VOC_{PAMS}$. The loaded tubes were analyzed using a thermal

84  desorption and gas chromatography/mass spectrometry (TD-GC/MS) method. In previous developmental

85  work, humidity and temperature during sampling were found to impact significantly on the analyses; for

86  this study, all sample collections were made under optimized conditions (Ho et al., 2017; Ho et al., 2018).

87  Sixteen airborne carbonyls (including mono- and dicarbonyls) were collected over diurnal cycles (i.e.,

88  20:00–08:00 local time [LT] and 08:00-20:00 LT) by 2,4-dintrophenyhydrozine (DNPH) coated-cartridges.

89  Detailed sampling and analytical procedures for VOCs and carbonyls can be found in previous publication

90  (Ho et al., 2017; Dai et al., 2012).

91  PM$_{2.5}$ filter samples were sampled with mini-volume samplers (Model Mini-Vol, Air Metrics Co.,

92  Oregon, USA) by a flow rate of 5 L min$^{-1}$ (Cao et al., 2005). Fine PM was sampled by 47-mm quartz

93  microfiber filters (Whatman QM/A, Maidstone, UK), and the filters were pre-heated at 900°C for 3-h

94  before sampling. The loaded filters were transfered into clean polystyrene petri dishes and stored in a

95  freezer.

96  **2.3 Chemical Analyses**

97  Analytical procedures for VOC analysis have been described previously (Ho et al., 2017). In brief, the

98  analytes in the adsorbent tubes were firstly desorbed in a thermal desorption unit (Series 2 UNITY-xr

99  system with ULTRA-xr, Markes International, Ltd., UK) coupled to a GC/MS (7890A/5977B, Agilent

100  Technologies, Santa Clara, CA, USA). The loaded tube was transfered into the TD unit and blown with

101  ultra-high purity He gas. The targeted VOCs were desorbed at 330°C within 8 mins, and then refocused

102  onto a cryogenic-trap (U-T1703P-2S, Markes) at −15°C.  The targeted VOCs were transfered to a cold

103  GC capillary column head (Rtx®-1, 105 m × 0.25 mm × 1 mm film thickness, Restek Corporation, USA) at

104  −45°C. The chromatographic condition could be found in our previous work (Ho et al., 2017).

105  For carbonyl compounds, the DNPH cartridges were firstly eluted with acetonitrile (HPLC/GCMS

106  grade, J & K Scientific Ltd., Ontario, Canada) (Dai et al., 2012). The extracts were analyzed with a typical

107  high-pressure liquid chromatography (HPLC) system (Series 1200; Agilent Technologies) equipped with

108  photodiode array detector. The column was matched with a 4.6 × 250 mm Spheri-5 ODS 5 μm C-18

109  reversed-phase column (Perkin-Elmer Corp., Norwalk, CT) (Dai et al., 2012; Ho et al., 2011).

110  The particulate organic carbon (OC) and elementary carbon (EC) were analyzed with a DRI model 2001

111  carbon analyzer (Atmoslytic, Inc., Calabasas, CA, USA) (Chow et al., 2007; Chow et al., 1993). Anions

112  (Cl$^-$, NO$_3^-$, and SO$_4^{2-}$) and cations (Na$^+$, NH$_4^+$, K$^+$, Mg$^{2+}$, and Ca$^{2+}$) in particles were determined in

113  aqueous extracts of the sample filters. Detailed extraction and analytical procedures were presented in a

114    previous publication (Zhang et al., 2011). The abundances of 25 particulate elements (Na, Mg, Al, Si, S,

115    Cl, K, Ca, Sc, Ti, V, Cr, Mn, Fe, Co, Ni, Cu, As, Se, Br, Sr, Ba, Pb, Ga, Zn)   were measured by energy

116    dispersive x-ray fluorescence (ED-XRF) spectrometry (Epsilon 4 ED-XRF, PAN alytical B.V., the

117    Netherlands). The X-ray source was matched with a metal-ceramic X-ray tube with a Rh and Ag anode,

118    and X-ray source was operated at a maximum current of 3mA, and the maximum accelerating voltage of

119    50kV (maximum power 15W).

120    **2.4 Quality Control**

121    The Minimum detection limits (MDLs) of the VOCs were in the range of 0.003–0.042 ppbv with a 3 L

122    sampling volume (Table S1). The measurement precision at 2 ppbv was $\leq$ 5%(Ho et al., 2017;Ho et al.,

123    2018). Three field blank samples were collected within each sampling day, and they were analyzed using

124    the same procedures as those for the ambient air samples. Most target compounds were not detected in the

125    field blanks, and propylene, benzene, and toluene were below their MDLs (< 0.23 g per tube and < 10% of

126    the arithmetic mean of ambient samples). No breakthrough (~0%) was observed for VOCs$_{PAMS}$ except for

127    $C_2$–$C_3$ hydrocarbons, which were < 10% when the air temperature was > 30°C. The MDLs for the carbonyl

128    target compounds were between 0.009 to 0.067 ppbv at a sampling volume of 3.6 m$^3$. Negligible

129    breakthrough (< 5%) was found under the sampling conditions and flow rates in the field.

130    **3. Results and Discussion**

131    **3.1 Origins of ambient VOCs during Dust and Fine-particle Pollution Events**

132    In the present study, mixing ratios of the sum of non-methane hydrocarbon was 36.0±15.7ppbv, which

133    was lower comparing to that in Beijing and Guangzhou with values of 51.0 and 47.8 ppbv, respectively.

134    Similar levels of alkenes were seen at the cities of Beijing (9.4 ppbv) and Guangzhou (8.2 ppbv)

135    comparing to that in the present study (9.2 ppbv, Table S2, Ho et al., 2004;Liu et al., 2008b).

136    Unexpectedly, the aromatics were slightly higher in Xi'an (10.3 ppbv) than that in Beijing (9.6 ppbv),

137    and 50% higher than that in Guangzhou (6.8 ppbv, Shao et al., 2009;Zou et al., 2015). Therein, ethylene,

138    ethane, toluene, iso-pentane, propane, n-butane, iso-butane, propylene, n-pentane, and benzene were the

139    most 10 abundant VOCs$_{PAMS}$. The high fractions of these markers reflect strong emissions from traffic

140    and coal combustion or from biomass burning (Liu et al., 2008a; Ho et al., 2009; Huang et al., 2015; Fan

141 et al., 2014; Zhang et al., 2015c). Previous studies found higher contributions of non-fossil sources to

142 carbonaceous aerosols in Xi'an, as compared with Beijing (Ni et al., 2018). Generally, non-fossil

143 emissions mainly originate from biomass burning (Ni et al., 2018), and the higher contribution of

144 non-fossil sources to carbonaceous in Xi'an would indicate remarkable biomass burning activities exist

145 in Xi'an and the surrounding areas (Huang et al., 2014; Xu et al., 2016).

146     Receptor models and correlations between individual VOCs have been used for source assessments. In

147 this study, significant correlation ($R^2$=0.62, p<0.05, slope of 1.59) was found for a least-squares

148 regression between toluene and benzene (Figure S1). The ratio of toluene to benzene (T/B) ratio has been

149 shown to different among combustion sources; for example, Liu et al. (2006) reported T/B ratios of

150 1.5-2.0 in gasoline-related emissions collected in a tunnel. In contrast, T/B ratios ranged from 0.23-0.68

151 and 0.13-0.71 for biomass burning and coal combustion, respectively (Zhang et al., 2015c). The T/B

152 ratios in our samples ($R^2$=0.62, p<0.05, slope of 1.59) implied a strong impact from traffic on the

153 ambient VOCs in Xi'an. Significant correlations (p<0.05) were observed among $C_3$-$C_5$ alkanes, with

154 propane versus n-butane ($R^2$=0.75, slope=0.91), n-pentane versus iso-pentane ($R^2$=0.85, slope=0.35), and

155 trans-2-butene versus cis-2-butene ($R^2$=0.99, slope=0.84)(Figure S1). The observed ratio of propane to

156 n-butane in Xi'an was 1.1, which is close to that (1.36) observed in the tunnel study cited above (Liu et

157 al., 2008). High loadings of n-pentane and iso-pentane are indicative of unburned vehicular emissions,

158 and Liu et al., (2008) reported a ratio of iso-pentane/n-pentane of 3 in tunnel air, which is consistent with

159 the slope of 2.85 found in the present study. The ratios of T/B, trans-/cis-2-butene, propane/n-butane and

160 n-pentane/iso-pentane indicated that gasoline emission was dominated sources of ambient VOCs, and the

161 source apportionment by PMF model result, and the detail description of source apportionment will be

162 carried out in the following section.

163     PMF model was used to identify the major pollution sources: the data input to the model were the

164 mixing ratios and uncertainties in the VOCs mixing ratios for all valid samples collected during the study.

165 Five sources were identified (Figure S2), and the detail process of source apportionment were given in

166 the supporting information. Biomass burning and gasoline exhaust were the two most significant pollution

167 sources, contributing 24.76% and 18.37%, respectively. The combustion of LPG and CNG (24.67%),

168 diesel exhaust (15.28%), coal combustion (16.92%) also were found to be important sources of ambient

169 VOCs (Figure S2). Biomass is commonly used for heating and cooking in rural areas of the basin in winter

170 due to its low cost compared with natural gas and electricity. Consistent with our results, previous studies

171    found high contribution of biomass burning and gasoline exhaust to the organic aerosol in Guanzhong

172    Basin(Cao et al., 2005).

173    Clear air conditions occurred at the beginning of the sampling period, but severe dust and fine-particle

174    pollution events were observed afterward. The high dust event was defined by loading of particulate

175    matter $\leq$10 μm in aerodynamic diameter ($PM_{10}$) between 300 and 500 μg m$^{-3}$, and these conditions

176    occurred from 12:00 LT on 9 November to 13:00 LT on 10 November. The abatement of dust before the

177    fine particle pollution event is referred to as the transition period (i.e., $PM_{10}$ < 300 μg m$^{-3}$ and $PM_{2.5}$ <

178    100 μg m$^{-3}$). The loading of $PM_{2.5}$ subsequently increased, and heavy fine particle pollution ($PM_{2.5}$ > 100

179    μg m$_{-3}$) occurred after 18:00 LT on 11 November.

180    Ratios of individual VOCs can be used to identify the origins of the compounds and to study

181    atmospheric aging processes due to the special composition of VOCs in a typical source and the different

182    lifetime of VOCs species (Xue et al., 2017; Zhang et al., 2015c). In addition, influences from

183    meteorological variation and atmospheric transport also need to be considered when the potential sources

184    of the compounds in ambient air are characterized. To investigate the impacts of air mass transport on

185    VOCs concentrations, we calculated air-mass back trajectories using the NOAA HYSPLIT model for the

186    dust event (Figure S4a) and for the fine-particle pollution episode (Figure S4b). The trajectories were

187    calculated at an arrival height of 500 m above ground at the observation site. In view of the short

188    atmospheric lifetimes of VOCs (for example, isoprene, ~1.4 h; propylene, ~5.3 h; toluene, 2.1 d)

189    (Atkinson and Arey, 2003), 24-h back trajectories were used for this assessment.

190    Clear different air masses back trajectories and VOCs ratios were observed between dust pollution and

191    haze pollution periods. From 9 November to 10 November (in dust pollution period), the air mass

192    reaching Xi'an passed over areas to the west of the city (i.e., Gansu Province and Ningxia Autonomous

193    Region) through long range transport; after 11 November (formation of haze), the transport of air mass

194    was mainly limited to areas around southern Xi'an. Differences in the chemical compositions of ambient

195    VOCs in the dusty versus in the haze event can clearly be seen (Figure 2) in the ratios of toluene to

196    benzene (T/B, Toluene, $K_{OH}$ $5.96\times10^{-12}$ cm$^3$ molecule$^{-1}$ s$^{-1}$, Bencene, $K_{OH}$ $1.22\times10^{-12}$ cm$^3$ molecule$^{-1}$

197    s$^{-1}$) and m, p-xylene to ethylbenzene (X/E, m-xylene, $K_{OH}$ $2.30\times10^{-11}$ cm$^3$ molecule$^{-1}$ s$^{-1}$, p-xylene, $K_{OH}$

198    $1.43\times10^{-11}$ cm$^3$ molecule$^{-1}$ s$^{-1}$, ethylbenzene, $K_{OH}$ $7.00\times10^{-12}$ cm$^3$ molecule$^{-1}$ s$^{-1}$). During the clear and

199    dusty periods, the T/B and X/E ratios varied significantly with time of day; that is, the highest values for

200    T/B (4.5–9.0) and X/E (0.98–1.05) were seen during rush hour (07:00–09:00 LT and 17:00–19:00 LT),

201    while the lowest values (0.50–1.95 for T/B, and 0.89–0.96 for X/E) occurred in the early afternoon (i.e.,

202    14:00–15:00 LT). The timings of the high T/B and X/E ratios suggest that fresh emissions from local

203    traffic were the major source for the ambient VOCs, and this implies that long-range transport did not

204    have a strong impact on the ambient VOCs during the clear or dusty parts of the study (Ho et al., 2004;

205    Liu et al., 2008a). While during the transitional and fine PM pollution period, both T/B and X/E varied

206    but at relatively lower values compared with the earlier parts of the study (T/B, 3.33±1.97, 2.21±0.86,

207    1.91±0.74, 2.01±0.56 in clear, dust, transitional and fine particle pollution periods, respectively; X/E,

208    1.00±0.05, 1.05±0.12, 0.93±0.17, 0.95±0.13 in clear, dust, transitional and fine particle pollution periods,

209    respectively). These synchronous lower values of T/B and X/B in transitional and fine particle pollution

210    periods were indicative of aged air masses (Zhang et al., 2015c; Xue et al., 2017; Warneke et al., 2013).

211       Variations in the air mass transport pathway, and T/B or X/E during different sampling periods (clear,

212    dust, transitional, fine particle pollution) confirmed that ambient VOCs were fresh in the clear and dust

213    periods, but relatively aged during the transitional and fine particle pollution periods(Zhang et al., 2015c;

214    Xue et al., 2017; Warneke et al., 2013). This indicates that the long-range transport of air mass had a

215    relatively weak influence on the ambient VOCs even during the high dust period. Otherwise,

216    composition of ambient VOCs should be relative aged due to long exposure time with dust transport.

217    Indeed, emissions from local vehicular exhausts and biomass burning in Xi'an and the surrounding areas

218    were the main contributors to ambient VOCs throughout our study.

219    **3.2 Transformation of VOCs between Dust and Fine Particle Events**

220       With the shading of dust, level of ambient VOCs decreased with time, and the low concentrations (8.3

221    to 33.9 ppbv) were observed from 13:00 LT on 10 November and 01:00 LT on 11 November (Figure 3).

222    During the fine particle pollution period (12–13 November), the $\sum VOCs_{PAMS}$ increased, reaching an

223    average of 38.0 ppbv in the last 24 h, compared with 19.0 ppbv in the transitional period and 21.5 ppbv

224    in the first 12 h of the fine particle pollution episode (Figure 3). This buildup of VOCs can be explained

225    by weak dispersion and relatively shallow boundary layers (400–1000 m) during the event (Figure 3). In

226    addition, during this transition period, much lower ratios of T/B and X/E were observed in comparison

227    with those in other periods (as mentioned in the part 3.1.2). We propose the possibility that windblown

228    dust which include sustainable $TiO_2$ can influence the atmospheric photochemistry of VOCs, which

229    would accelerate the oxidation of ambient VOCs (Chu et al. 2019; Nie et al., 2014).

230  While changes in the emission sources and their strengths, physical dispersion, regional transport, and

231  aging of air masses all could affect VOC levels and composition (Xue et al., 2013; Xue et al., 2017). As a

232  result, to evaluated aging of ambient VOCs in different period, the impact of dust on the transform of

233  ambient VOCs, and the relative processes, the mentioned factors should be fully considered.

234  To evaluate the impact of sources types on the variation of VOCs in the dust-to-haze episode, diurnal

235  variation of VOCs was depicted. During the clear and dusty periods—and similar to the trends in T/B

236  and X/E ratios—peaks in $\sum \mathrm{VOC_{SPAMS}}$ were seen from 17:00 to 20:00 LT and from 09:00 to 12:000 LT

237  (Figure 3), which highlighted the impacts of local traffic emission (Liu et al., 2008a; Huang et al., 2015).

238  And 1,3-Butadiene is often used as marker of gasoline-powered motor vehicles (Huang et al., 2015),

239  while ethane is key chemical marker for biomass and coal combustion (Liu et al., 2008a). Time series

240  plots of 1,3-butadiene and ethane (Figure S5) show that peaks in 1,3-butadiene mostly occurred during

241  rush hour, while higher concentrations of ethane were seen during the night. These results support the

242  conclusions that there were strong impacts from gasoline-powered motor vehicles in the daytime and

243  from biomass burning or coal combustion for heating at night. In addition, winter heating activities was

244  relatively active because of low temperatures during the transitional period, and this limited the

245  possibility of reduced emission amounts. Hence the variations of sources strength was eliminated from

246  the major factor caused the extremely low concentration and relative aged composition of ambient

247  VOCs.

248  Variation of physical dispersion was also eliminated. With the shading of dust transport, shallow

249  boundary layers were observed in the transitional period. For the clear and dust transport period, the

250  boundary layer between 08:00 to 14:00 was relatively deep (1150–1500 m). In contrast, the boundary

251  layer height decreased sharply to < 800 m on 11 November in transitional period. This limited the

252  possibility that diffusion caused the sharp decrease of ambient VOCs in the transitional period.

253  Significant impact of air mass input was eliminated. Input of air mass would certainly cause the

254  variations of VOCs' composition and loading (Xue et al., 2014). In the present study, long range

255  transport of air masses had limited impacts on the characteristic of ambient VOCs during the sampling

256  period. In another aspect, relative active VOCs would be firstly degraded, hence composition of ambient

257  VOCs would be aging with long range transport (Ho et al., 2009; Xue et al., 2017). While in the present

258  study, as mentioned above, composition of ambient VOCs was relative fresh under long range transport

259  of air mass (within dust transport). In contrast, VOCs composition was relatively aged under the air mass

260  that limited with Xi'an and the surrounding area (transitional period). This phenomenon indicated that

261  regional transport cannot be the major factor inducing the relative aged composition and excess low

262  loading of the ambient VOCs in the transitional period.

263  Synchronous changes of the VOCs isomeride were found in the windblown dust-to-haze episode,

264  which supplied the evidence of the accelerated photochemistry reactions. In the present study, we

265  found fast decrease of trans-/cis-2-butene ratio within dust transporting, which confirmed the accelerated

266  photochemical reactions of ambient VOCs (Figure 4). Trans-2-butene and cis-2-butene are two

267  isomerides that mostly emitted from same sources (Zheng et al., 2017; Zhang et al., 2015b). While

268  trans-2-butene has higher photochemical reactions rate with OH radical in the atmosphere ($k_{OH}$

269  $6.40 \times 10^{-11}$ $cm^3$ $molecule^{-1}$ $s^{-1}$) than cis-2-butene ($k_{OH}$ $5.64 \times 10^{-11}$ $cm^3$ $molecule^{-1}$ $s^{-1}$) (Perring et al.,

270  2013), hence trans-/cis-2-butene ratio would decrease with the photochemical reactions (Zhang et al.,

271  2015b). Firstly, relative higher trans-/cis-2-butene ratios were observed in the rush hours (evening rush

272  hours 17:00-20:00, morning rush hours 07:00-10:00) (Figure 4), which indicated fresh emission from

273  local traffic activities (Zhang et al., 2015b). In addition, sharp decrease of trans-/cis-2-butene ratio was

274  observed from late half of windblown dust period to the end of transitional period (Figure 4). The quickly

275  shrinking of trans-2-butene comparing to cis-2-butene in the dust pollution period indicated that

276  oxidation of ambient VOCs was accelerated in the period with high loading of the suspending dust

277  particles (Zhang et al., 2015b).

278  Significant increase of particulate active metals was found in dust pollution period, which further

279  verified the promotion of dust on the heterogeneous reactions. Previous study found that mineral dust can

280  affect the chemistry of the atmosphere by scavenging gaseous compounds (Zhang et al., 2000;Chen et al.,

281  2012); it can also promote heterogeneous reactions of atmospheric substances, including VOCs, because

282  the particle surfaces can provide sites for photo-catalytic reactions (Cwiertny et al., 2008;Ndour et al.,

283  2009). In the present study, ferrum (Fe) and titanium (Ti) contents of the particulate increased

284  significantly within the period with dust transport (Figure 5). In detail, content of Fe increased from 19.3

285  $\mu g$ $m^{-3}$ in clear days to 40.8 $\mu g$ $m^{-3}$ in dust pollution days, and the content of Ti increased from 0.92 to

286  2.98 $\mu g$ $m^{-3}$. Hence, huge increase of the Ti and Fe concentrations in particulate phase during the period

287  of dust pollution days could possibly promote the gas-solid photochemical reaction of the ambient VOCs,

288  which would reasonably ascribe the relative low level and aged composition of ambient VOCs in this

289  period(Chu et al., 2019; He et al., 2014;Song et al., 2019).

**3.3 Variation of carbonyl compounds between dust to fine particle pollution periods: further formation oxygenated VOCs with aging of primary VOCs**

Aging of primary VOCs and formation of carbonyl compounds were observed synchronously, as the fine-particle pollution event developed (Figure 3; Figure 6a). As discussed above, relatively low T/B and X/E values were observed during the transitional and fine PM periods after the dust event (Part 3.2). In our study, the carbonyl levels increased after the clear and dusty periods, and the highest levels were seen during the fine particle pollution event (Figure 6a). Carbonyl compounds are produced from both the primary sources and form through secondary processes (Dai et al., 2012; Duan et al., 2012), and we found higher carbonyl concentrations during daytime than at night (Figure 6a). This is consistent with previous studies in Xi'an (Dai et al., 2012), which confirmed the secondary formation of carbonyl compound under sunlight illumination.

Methylglyoxal is generally considered to be a secondary species, while acetone is mainly from primary emissions; the ratio of acetone to methylglyoxal (A/M) has been used as an indicator of air mass aging (Dai et al., 2012; Liu et al., 2006). In the present study, A/M ranged from 12 to 14 during the clear and first half of dusty periods but then dropped sharply and stayed between 6 and 9 during the later parts of dust pollution period, transitional and the high PM event (Figure 6a). Increases in the abundances of carbonyl compounds and lower A/M ratios suggested relatively stronger aging of the air masses, this is further evidence of fast degradation of VOCs in the late half of the windblown dust event, and the primary VOCs were oxidized and served as precursors of SOA. In consequence, composition of particles changed with oxidation of ambient VOCs across the sampling periods.

**3.4 Variations of PM$_{2.5}$ Chemical Composition during Dusty and Fine PM Pollution Periods**

Significant variations of water-soluble inorganic ions, OC, and EC were observed diurnally and between dust and fine particle pollution events (Figure 6b, c). For instance, the concentrations of $NO_3^-$ were relatively high in the daytime, while $K^+$ and $Cl^-$ were more abundant at night. The diurnal cycles can be explained by the formation of secondary particles through photochemical processes during the daytime and by the impacts from biomass and coal burning for heating at night (Dai et al., 2012;Zhang et al., 2018;Cong et al., 2015). The concentrations of $Ca^{2+}$, $Mg^{2+}$, and $Na^+$, which are typically associated with dust in inland areas (Wu et al., 2011), increased sharply during the dusty period, and then declined rapidly afterwards.

319    As discussed, the apparent contribution of VOCs to the formation of SOAs increased when the dusty

320    conditions transitioned into a fine-particle pollution event. Temporal changes in the chemical

321    composition of $PM_{2.5}$ are consistent with this suggestion. During the fine-particle pollution period, both

322    the concentrations of secondary ions, particularly $NO_3^-$, increased as the haze event developed. A similar

323    trend was seen for OC (Figure 6b), and content of particulate OC increased from 11.1 μg m$^{-3}$ since dust

324    event period to 47.1 μg m$^{-3}$ in the haze period. In another aspect, the ratio of OC/EC increased from 1.3

325    to 4.9 in the dust-to-haze episode. The previous studies on the characterization of particles from traffic

326    emission reported OC/EC values in the range of 0.28 to 0.92 in the diesel vehicles, and the OC/EC values

327    were reported >2 in the gasoline vehicles (Cadle et al., 1999; Huang et al., 2006). In addition, the OC/EC

328    was reported in the range of 0.9 to 1.6 in the urban region in the city of Guangzhou (Tao et al., 2019). In

329    the present study, the consistent increase of OC/EC would prove the formation of SOA in the

330    dust-to-haze episode. Combined with the findings regarding the compositions of VOCs and $PM_{2.5}$, these

331    results indicate that the reactions of VOCs led to the formation of SOA, and in so doing contributed to

332    the fine particle pollution.

333    **4. Conclusion**

334    Comprehensive field work was carried out to investigate the origin and transform of VOCs within the

335    dust-fine particles pollution periods in winter with the city of Xi'an. And the assumption of promotions

336    of dust on the heterogeneous reactions of VOCs was further verified. Local vehicle exhaust and heating

337    activities were found to be the most important sources of the ambient VOCs in Xi'an within winter,

338    while long range transport air mass has limited impacts. Within the period of dust transport, loading of

339    ambient VOCs decreased sharply from the late half period, and the lowest concentration was observed in

340    the transitional period, in accordance with aging of primary VOCs. In addition, loading and proportion of

341    secondary VOCs in gaseous phase and secondary ions and organic carbon in particulate phase increased

342    with the aging of primary VOCs. Source strength, physical dispersion, and regional transport were

343    eliminated from the major factor for the variation of the ambient VOCs. On another aspect, sharp

344    increase of active metals concentrations (Ti and Fe) and fast decrease of trans-/cis-2-butene ratio were

345    observed from the late half of dust transport period. In consequence, we conclude that windblown dust

346　　might accelerate the gas-solid heterogeneous reactions of atmospheric VOCs, and further induced the

347　　formation of SOA precursors.

348

349　　*Data availability.* All of the research data have been included in the supplement.

350

351　　*Supplement.* The following information is provided in the Supplement: Sampling procedures, Chemical

352　　Analysis, Source characterization, Figure S1-S5, Table S1-S2.

353

354　　*Author contributions.* YX designed the study. YX and YH wrote the paper. SH, JC and SL revised the

355　　manuscript, LC and LW analyzed the data. All authors reviewed and commented on the paper.

356

357　　*Competing interests.* The authors declare that they have no conflict of interest.

358

363　　**References**

364　　Atkinson, R., and Arey, J.: Atmospheric Degradation of Volatile Organic Compounds, Chem. Rev., 103,

365　　4605-4638, https://doi.10.1021/cr0206420, 2003.

366　　Cadle SH, Mulawa PA, Hunsanger EC, Nelson K, Ragazzi RA, Barrett R.: Composition of light-duty

367　　motor vehicle exhaust particulate matter in the Denver, Colorado area. Environ. Sci. Technol., 33:

368　　2328-2339, https://doi.org/10.1021/es9810843, 1999.

369　　Cao, J., Wu, F., Chow, J., Lee, S., Li, Y., Chen, S., An, Z., Fung, K., Watson, J., and Zhu, C.:

370　　Characterization and source apportionment of atmospheric organic and elemental carbon during fall and

371　　winter of 2003 in Xi'an, China, Atmos. Chem. Phys., 5, 3127-3137, https://doi.

372　　org/10.5194/acp-5-3127-2005, 2005.

373    Chen, H., Nanayakkara, C. E., and Grassian, V. H.: Titanium Dioxide Photocatalysis in Atmospheric

374    Chemistry, Chem. Rev., 112, 5919-5948, https://doi.10.1021/cr3002092, 2012.

375    Chow, J. C., Watson, J. G., Pritchett, L. C., Pierson, W. R., Frazier, C. A., and Purcell, R. G.: The dri

376    thermal/optical reflectance carbon analysis system: description, evaluation and applications in U.S. Air

377    quality studies, Atmos. Environ., Part A. General Topics, 27, 1185-1201,

378    https://doi.org/10.1016/0960-1686(93)90245-T, 1993.

379    Chow, J. C., Watson, J. G., Chen, L. W. A., Chang, M. C. O., Robinson, N. F., Trimble, D., and Kohl, S.:

380    The IMPROVE_A Temperature Protocol for Thermal/Optical Carbon Analysis: Maintaining Consistency

381    with a Long-Term Database, J. Air Waste Manage., 57, 1014-1023,

382    https://doi.org/10.3155/1047-3289.57.9.1014, 2007.

383    Chu, B., Wang, Y., Yang, W., Ma, J., Ma, Q., Zhang, P., Liu, Y., and He, H.: Effects of $NO_2$ and $C_3H_6$

384    on the heterogeneous oxidation of $SO_2$ on $TiO_2$ in the presence or absence of UV irradiation, Atmos.

385    Chem. Phys. Discuss., 2019, 1-20, https://doi.org/10.5194/acp-2019-532, 2019.

386    Cong, Z., Kang, S., Kawamura, K., Liu, B., Wan, X., Wang, Z., Gao, S., and Fu, P.: Carbonaceous

387    aerosols on the south edge of the Tibetan Plateau: concentrations, seasonality and sources, Atmos. Chem.

388    Phys., 15, 1573-1584, https://doi.org/10.5194/acp-15-1573-2015, 2015.

389    Cwiertny, D. M., Young, M. A., and Grassian, V. H.: Chemistry and photochemistry of mineral dust

390    aerosol, Annu. Rev. Phys. Chem., 59, 27-51, https://doi.

391    org/10.1146/annurev.physchem.59.032607.093630, 2008.

392    Dai, W. T., Ho, S. S. H., Ho, K. F., Liu, W. D., Cao, J. J., and Lee, S. C.: Seasonal and diurnal variations

393    of mono- and di-carbonyls in Xi'an, China, Atmos. Res., 113, 102-112,

394    http://dx.doi.org/10.1016/j.atmosres.2012.05.001, 2012.

395    Dentener, F. J., Carmichael, G. R., Zhang, Y., Lelieveld, J., and Crutzen, P. J.: Role of mineral aerosol as

396    a reactive surface in the global troposphere, J. Geophys. Res.-Atmos., 101, 22869-22889,

397    https://doi:10.1029/96JD01818, 1996.

398    Dickerson, R. R., Kondragunta, S., Stenchikov, G., Civerolo, K. L., Doddridge, B. G., and Holben, B. N.:

399    The Impact of Aerosols on Solar Ultraviolet Radiation and Photochemical Smog, Science, 278, 827,

400    https://doi:10.1126/science.278.5339.827, 1997.

401    Duan, J., Guo, S., Tan, J., Wang, S., and Chai, F.: Characteristics of atmospheric carbonyls during haze

402    days in Beijing, China, Atmos. Res., 114, 17-27, http://dx.doi.org/10.1016/j.atmosres.2012.05.010, 2012.

403     Fan, R., Li, J., Chen, L., Xu, Z., He, D., Zhou, Y., Zhu, Y., Wei, F., and Li, J.: Biomass fuels and coke

404     plants are important sources of human exposure to polycyclic aromatic hydrocarbons, benzene and

405     toluene, Environ. Res., 135, 1-8, http://dx.doi.org/10.1016/j.envres.2014.08.021, 2014.

406     Feng, T., Bei, N. F., Huang, R. J., Cao, J. J., Zhang, Q., Zhou, W. J., Tie, X. X., Liu, S. X., Zhang, T., Su,

407     X. L., Lei, W. F., Molina, L. T., and Li, G. H.: Summertime ozone formation in Xi'an and surrounding

408     areas, China, Atmos. Chem. Phys., 16, 4323-4342, http://doi.org/10.5194/acp-16-4323-2016, 2016.

409     Ginoux, P., Chin, M., Tegen, I., Prospero, J. M., Holben, B., Dubovik, O., and Lin, S. J.: Sources and

410     distributions of dust aerosols simulated with the GOCART model, J. Geophys. Res.-Atmos., 106,

411     20255-20273, http://doi.10.1029/2000jd000053, 2001.

412     Guo, S., Hu, M., Zamora, M. L., Peng, J. F., Shang, D. J., Zheng, J., Du, Z. F., Wu, Z., Shao, M., Zeng, L.

413     M., Molina, M. J., and Zhang, R. Y.: Elucidating severe urban haze formation in China, Proc. Natl. Acad.

414     Sci. USA, 111, 17373-17378, https://doi.org/10.1073/pnas.1419604111, 2014.

415     Guo, S., Hu, M., Lin, Y., Gomez-Hernandez, M., Zamora, M. L., Peng, J., Collins, D. R., and Zhang, R.:

416     OH-Initiated Oxidation of m-Xylene on Black Carbon Aging, Environ. Sci. Technol., 50, 8605-8612,

417     http://doi.org/10.1021/acs.est.6b01272, 2016.

418     He, H., Wang, Y. S., Ma, Q. X., Ma, J. Z., Chu, B. W., Ji, D. S., Tang, G. Q., Liu, C., Zhang, H. X., and

419     Hao, J. M.: Mineral dust and NOx promote the conversion of SO2 to sulfate in heavy pollution days, Sci.

420     Rep.-UK., 4, http://doi.10.1038/srep04172, 2014.

421     Ho, K. F., Lee, S. C., Guo, H., and Tsai, W. Y.: Seasonal and diurnal variations of volatile organic

422     compounds (VOCs) in the atmosphere of Hong Kong, Sci. Total. Environ., 322, 155-166,

423     http://dx.doi.org/10.1016/j.scitotenv.2003.10.004, 2004.

424     Ho, K. F., Lee, S. C., Ho, W. K., Blake, D. R., Cheng, Y., Li, Y. S., Ho, S. S. H., Fung, K., Louie, P. K.

425     K., and Park, D.: Vehicular emission of volatile organic compounds (VOCs) from a tunnel study in Hong

426     Kong, Atmos. Chem. Phys., 9, 7491-7504, http:// doi.org/10.5194/acp-9-7491-2009, 2009.

427     Ho, S. S. H., Ho, K. F., Liu, W. D., Lee, S. C., Dai, W. T., Cao, J. J., and Ip, H. S. S.: Unsuitability of

428     using the DNPH-coated solid sorbent cartridge for determination of airborne unsaturated carbonyls,

429     Atmos. Environ., 45, 261-265, http:// doi.org/10.1016/j.atmosenv.2010.09.042, 2011.

430     Ho, S. S. H., Chow, J. C., Watson, J. G., Wang, L., Qu, L., Dai, W., Huang, Y., and Cao, J.: Influences of

431     relative humidities and temperatures on the collection of C2-C5 aliphatic hydrocarbons with multi-bed

432    (Tenax TA, Carbograph 1TD, Carboxen 1003) sorbent tube method, Atmos. Environ., 151, 45-51,

433    http://dx.doi.org/10.1016/j.atmosenv.2016.12.007, 2017.

434    Ho, S. S. H., Wang, L., Chow, J. C., Watson, J. G., Xue, Y., Huang, Y., Qu, L., Li, B., Dai, W., Li, L.,

435    and Cao, J.: Optimization and evaluation of multi-bed adsorbent tube method in collection of volatile

436    organic compounds, Atmos. Res., 202, 187-195, https://doi.org/10.1016/j.atmosres.2017.11.026, 2018.

437    Huang, R., Zhang, Y., Bozzetti, C., Ho, K., Cao, J., Han, Y., Daellenbach, K. R., Slowik, J. G., Platt, S.

438    M., Canonaco, F., Zotter, P., Wolf, R., Pieber, S. M., Bruns, E. A., Crippa, M., Ciarelli, G., Piazzalunga,

439    A., Schwikowski, M., Abbaszade, G., Schnelle-Kreis, J., Zimmermann, R., An, Z., Szidat, S.,

440    Baltensperger, U., Haddad, I. E., and Prevot, A. S. H.: High secondary aerosol contribution to particulate

441    pollution during haze events in China, Nature, 514, 218-222, https://doi.org/10.1038/nature13774, 2014.

442    Huang X, Yu J, He L, Hu M.: Size distribution characteristics of elemental carbon emitted from Chinese

443    vehicles: Results of a tunnel study and atmospheric implications. Environ. Sci. Technol., 40: 5355-5360,

444    https://doi.org/10.1021/es0607281, 2006.

445    Huang, Y., Ling, Z. H., Lee, S. C., Ho, S. S. H., Cao, J. J., Blake, D. R., Cheng, Y., Lai, S. C., Ho, K. F.,

446    Gao, Y., Cui, L., and Louie, P. K. K.: Characterization of volatile organic compounds at a roadside

447    environment in Hong Kong: An investigation of influences after air pollution control strategies, Atmos.

448    Environ., 122, 809-818, http://dx.doi.org/10.1016/j.atmosenv.2015.09.036, 2015.

449    Li, B., Ho, S. S. H., Xue, Y., Huang, Y., Wang, L., Cheng, Y., Dai, W., Zhong, H., Cao, J., and Lee, S.:

450    Characterizations of volatile organic compounds (VOCs) from vehicular emissions at roadside

451    environment: The first comprehensive study in Northwestern China, Atmos. Environ., 161, 1-12,

452    https://doi.org/10.1016/j.atmosenv.2017.04.029, 2017.

453    Liu, W., Zhang, J., Kwon, J., Weisel, C., Turpin, B., Zhang, L., Korn, L., Morandi, M., Stock, T., and

454    Colome, S.: Concentrations and Source Characteristics of Airborne Carbonyl Compounds Measured

455    Outside Urban Residences, J. Air Waste Manage., 56, 1196-1204,

456    https://doi.org/10.1080/10473289.2006.10464539, 2006.

457    Liu, Y., Shao, M., Fu, L., Lu, S., Zeng, L., and Tang, D.: Source profiles of volatile organic compounds

458    (VOCs) measured in China: Part I, Atmos. Environ., 42, 6247-6260,

459    http://dx.doi.org/10.1016/j.atmosenv.2008.01.070, 2008a.

460 Liu, Y., Shao, M., Lu, S., Chang, C.-C., Wang, J.-L., and Fu, L.: Source apportionment of ambient

461 volatile organic compounds in the Pearl River Delta, China: Part II, Atmos. Environ., 42, 6261-6274,

462 https://doi.org/10.1016/j.atmosenv.2008.02.027, 2008b.

463 Ndour, M., Conchon, P., D'Anna, B., Ka, O., and George, C.: Photochemistry of mineral dust surface as

464 a potential atmospheric renoxification process, Geophys. Res. Lett., 36, 4,

465 https://doi.org/10.1029/2008gl036662, 2009.

466 Ni, H., Huang, R., Cao, J., Liu, W., Zhang, T., Wang, M., Meijer, H. A. J., and Dusek, U.: Source

467 apportionment of carbonaceous aerosols in Xi'an, China: insights from a full year of measurements of

468 radiocarbon and the stable isotope C-13, Atmos. Chem. Phys., 18, 16363-16383,

469 https://doi.10.5194/acp-18-16363-2018, 2018

470 Nie, W., Ding, A. J., Wang, T., Kerminen, V. M., George, C., Xue, L. K., Wang, W. X., Zhang, Q. Z.,

471 Petaja, T., Qi, X. M., Gao, X. M., Wang, X. F., Yang, X. Q., Fu, C. B., and Kulmala, M.: Polluted dust

472 promotes new particle formation and growth, Sci. Rep.-UK., 4, 6, https://doi.org/10.1038/srep06634,

473 2014.

474 Perring, A. E., Pusede, S. E., and Cohen, R. C.: An Observational Perspective on the Atmospheric

475 Impacts of Alkyl and Multifunctional Nitrates on Ozone and Secondary Organic Aerosol, Chem. Rev.,

476 113, 5848-5870, https://doi.org/10.1021/cr300520x, 2013.

477 Shao, M., Lu, S. H., Liu, Y., Xie, X., Chang, C. C., Huang, S., and Chen, Z. M.: Volatile organic

478 compounds measured in summer in Beijing and their role in ground-level ozone formation, J. Geophys.

479 Res.-Atmos., 114, D00G06, https://doi.org/10.1029/2008jd010863, 2009.

480 Song, S. J., Gao, M., Xu, W. Q., Sun, Y. L., Worsnop, D. R., Jayne, J. T., Zhang, Y. Z., Zhu, L., Li, M.,

481 Zhou, Z., Cheng, C. L., Lv, Y. B., Wang, Y., Peng, W., Xu, X. B., Lin, N., Wang, Y. X., Wang, S. X.,

482 Munger, J. W., Jacob, D. J., and McElroy, M. B.: Possible heterogeneous chemistry of

483 hydroxymethanesulfonate (HMS) in northern China winter haze, Atmos. Chem. Phys., 19, 1357-1371,

484 https://doi.10.5194/acp-19-1357-2019, 2019.

485 Tao J, Zhang Z, Wu Y, Zhang L, Wu Z, Cheng P.: Impact of particle number and mass size distributions

486 of major chemical components on particle mass scattering efficiency in urban Guangzhou in southern

487 China. Atmos. Chem. Phys., 19, 8471-8490, https://doi.org/10.1021/es9810843, 2019

488 Warneke, C., de Gouw, J. A., Edwards, P. M., Holloway, J. S., Gilman, J. B., Kuster, W. C., Graus, M.,

489 Atlas, E., Blake, D., Gentner, D. R., Goldstein, A. H., Harley, R. A., Alvarez, S., Rappenglueck, B.,

490    Trainer, M., and Parrish, D. D.: Photochemical aging of volatile organic compounds in the Los Angeles

491    basin:    Weekday-weekend    effect,    J.    Geophys.    Res.-Atmos.,    118,    5018-5028,

492    http://doi.org/10.1002/jgrd.50423, 2013.

493    Wu, F., Chow, J. C., An, Z., Watson, J. G., and Cao, J.: Size-Differentiated Chemical Characteristics of

494    Asian Paleo Dust: Records from Aeolian Deposition on Chinese Loess Plateau, J. Air Waste Manage., 61,

495    180-189, 10.3155/1047-3289.61.2.180, 2011.

496    Xu, H., Cao, J., Chow, J. C., Huang, R. J., Shen, Z., Chen, L. W. A., Ho, K. F., and Watson, J. G.:

497    Inter-annual variability of wintertime PM2.5 chemical composition in Xi'an, China: Evidences of

498    changing    source    emissions,    Sci.    Total.    Environ.,    545,    546-555,

499    http://dx.doi.org/10.1016/j.scitotenv.2015.12.070, 2016.

500    Xue, L., Wang, T., Louie, P. K. K., Luk, C. W. Y., Blake, D. R., and Xu, Z.: Increasing External Effects

501    Negate Local Efforts to Control Ozone Air Pollution: A Case Study of Hong Kong and Implications for

502    Other Chinese Cities, Environ. Sci. Technol., 48, 10769-10775, 10.1021/es503278g, 2014.

503    Xue, L. K., Wang, T., Guo, H., Blake, D. R., Tang, J., Zhang, X. C., Saunders, S. M., and Wang, W. X.:

504    Sources and photochemistry of volatile organic compounds in the remote atmosphere of western China:

505    results    from    the    Mt.    Waliguan    Observatory,    Atmos.    Chem.    Phys.,    13,    8551-8567,

506    10.5194/acp-13-8551-2013, 2013.

507    Xue, Y., Ho, S. S. H., Huang, Y., Li, B., Wang, L., Dai, W., Cao, J., and Lee, S.: Source apportionment

508    of VOCs and their impacts on surface ozone in an industry city of Baoji, Northwestern China, Sci.

509    Rep.-UK., 7, 9979, https://doi.org/10.1038/s41598-017-10631-4, 2017.

510    Zhang, D. Z., Shi, G. Y., Iwasaka, Y., and Hu, M.: Mixture of sulfate and nitrate in coastal atmospheric

511    aerosols: individual particle studies in Qingdao (36 degrees 04 ' N, 120 degrees 21 ' E), China, Atmos.

512    Environ., 34, 2669-2679, http://doi.org/10.1016/s1352-2310(00)00078-9, 2000.

513    Zhang, D. Z., Zang, J. Y., Shi, G. Y., Iwasaka, Y., Matsuki, A., and Trochkine, D.: Mixture state of

514    individual Asian dust particles at a coastal site of Qingdao, China, Atmos. Environ., 37, 3895-3901,

515    http://doi./org/10.1016/s1352-2310(03)00506-5, 2003.

516    Zhang, N., Cao, J., Wang, Q., Huang, R., Zhu, C., Xiao, S., and Wang, L.: Biomass burning influences

517    determination based on PM2.5 chemical composition combined with fire counts at southeastern Tibetan

518    Plateau    during    pre-monsoon    period,    Atmos.    Res.,    206,    108-116,

519    https://doi.org/10.1016/j.atmosres.2018.02.018, 2018.

520    Zhang, Q., Shen, Z., Cao, J., Zhang, R., Zhang, L., Huang, R. J., Zheng, C., Wang, L., Liu, S., Xu, H.,

521    Zheng, C., and Liu, P.: Variations in PM2.5, TSP, BC, and trace gases (NO2, SO2, and O3) between

522    haze and non-haze episodes in winter over Xi'an, China, Atmos. Environ., 112, 64-71,

523    https://doi.org/10.1016/j.atmosenv.2015.04.033, 2015a.

524    Zhang, T., Cao, J. J., Tie, X. X., Shen, Z. X., Liu, S. X., Ding, H., Han, Y. M., Wang, G. H., Ho, K. F.,

525    Qiang, J., and Li, W. T.: Water-soluble ions in atmospheric aerosols measured in Xi'an, China: Seasonal

526    variations and sources, Atmos. Res., 102, 110-119, https://doi.org/10.1016/j.atmosres.2011.06.014, 2011.

527    Zhang, Y., Wang, X., Zhang, Z., Lu, S., Huang, Z., and Li, L.: Sources of C-2-C-4 alkenes, the most

528    important ozone nonmethane hydrocarbon precursors in the Pearl River Delta region, Sci. Total Environ.,

529    502, 236-245, https://doi.10.1016/j.scitotenv.2014.09.024, 2015b.

530    Zhang, Y., Bao, F., Li, M., Chen, C., and Zhao, J.: Nitrate-Enhanced Oxidation of SO2 on Mineral Dust:

531    A Vital Role of a Proton, Environ. Sci. Technol., 53, 10139-10145, https://doi.10.1021/acs.est.9b01921,

532    2019.

533    Zhang, Z., Wang, X., Zhang, Y., Lü, S., Huang, Z., Huang, X., and Wang, Y.: Ambient air benzene at

534    background sites in China's most developed coastal regions: Exposure levels, source implications and

535    health risks, Sci. Total Environ., 511, 792-800, http://dx.doi.org/10.1016/j.scitotenv.2015.01.003, 2015c.

536    Zheng Fang, W. D., Yanli Zhang, Xiang Ding, Mingjin Tang, Tengyu Liu, Qihou Hu, Ming Zhu, Zhaoyi

537    Wang, Weiqiang Yang, Zhonghui Huang, Wei Song, Xinhui Bi, Jianmin Chen, Yele Sun, Christian

538    George, and Xinming Wang: Open burning of rice, corn and wheat straws: primary emissions,

539    photochemical aging, and secondary organic aerosol formation, Atmos. Chem. Phys., 17, 14821-14839,

540    http://org/10.5194/acp-17-14821-2017, 2017.

541    Zou, Y., Deng, X., Zhu, D., Gong, D., Wang, H., Li, F., Tan, H., Deng, T., Mai, B., and Liu, X.:

542    Characteristics of 1 year of observational data of VOCs, NO x and O 3 at a suburban site in Guangzhou,
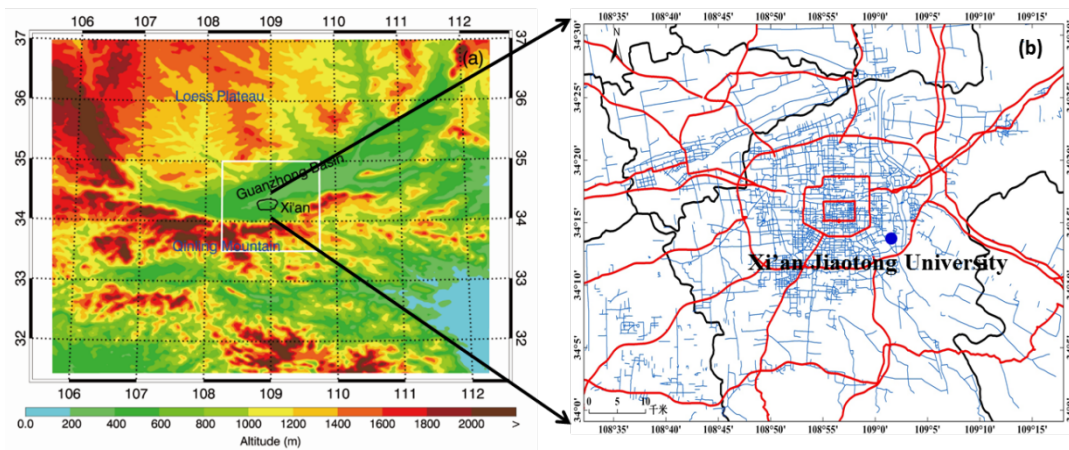
543    China, Atmos. Chem. Phys., 15, 6625-6636, https://doi.org/10.5194/acp-15-6625-2015, 2015.

544

545

546

547

548

549

550

551

552

553

554

555

556

557

558

559

560

561

562

563



564

**Figure 1: Regional and local maps of the study area, (a) Regional map showing the location of Xi'an and the surrounding geography; (b) local map of Xi'an showing the sampling site (blue dot), main roads (red lines), and secondary roads (blue lines).**
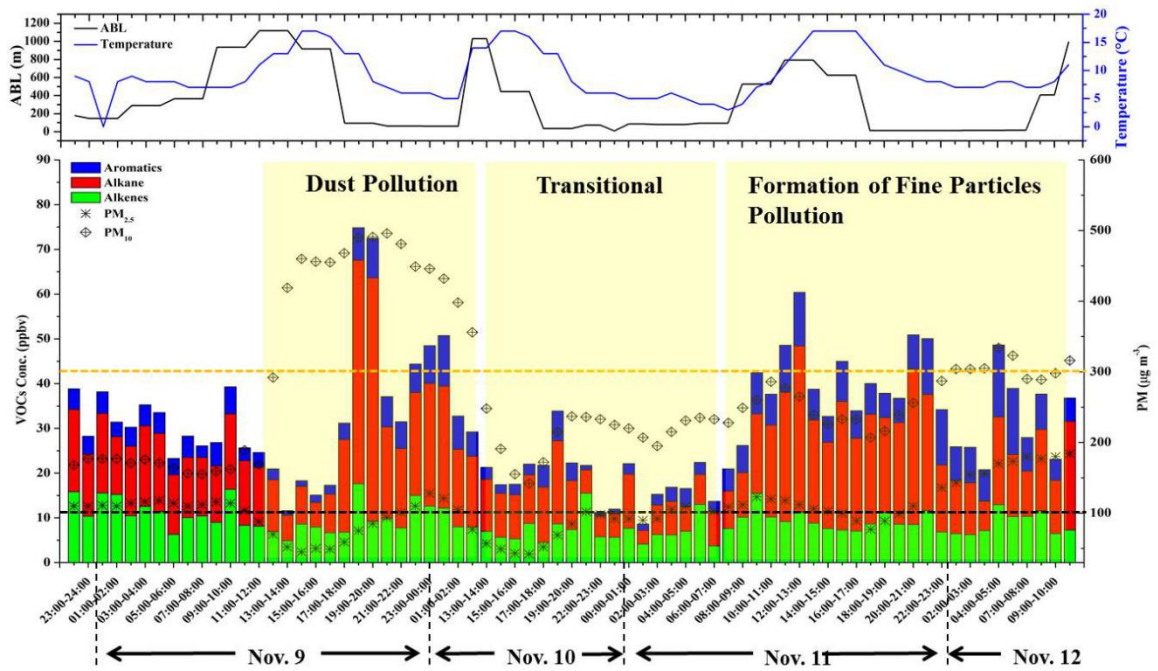
568

569

570

571

572

573

574

575

576

577

578

579

580

581

582

583

584

585

586



587
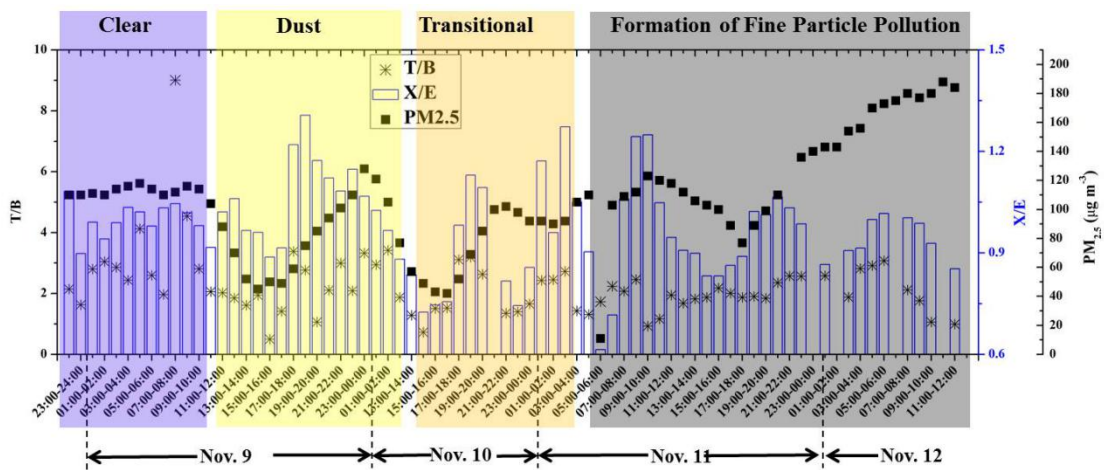
**Figure 2: Variations in the ratios of indicator volatile organic compound (VOC) species (toluene/benzene [T/B], and m-,p-xylene/ethylbenzene [X/E]) and fine particle loadings during the study period.**

590

591

592



593

**Figure 3: Temporal variations in volatile organic compound (VOC) concentrations and particle levels during the sampling period (9–13 November 2016).**

594
595

596

597

598

599
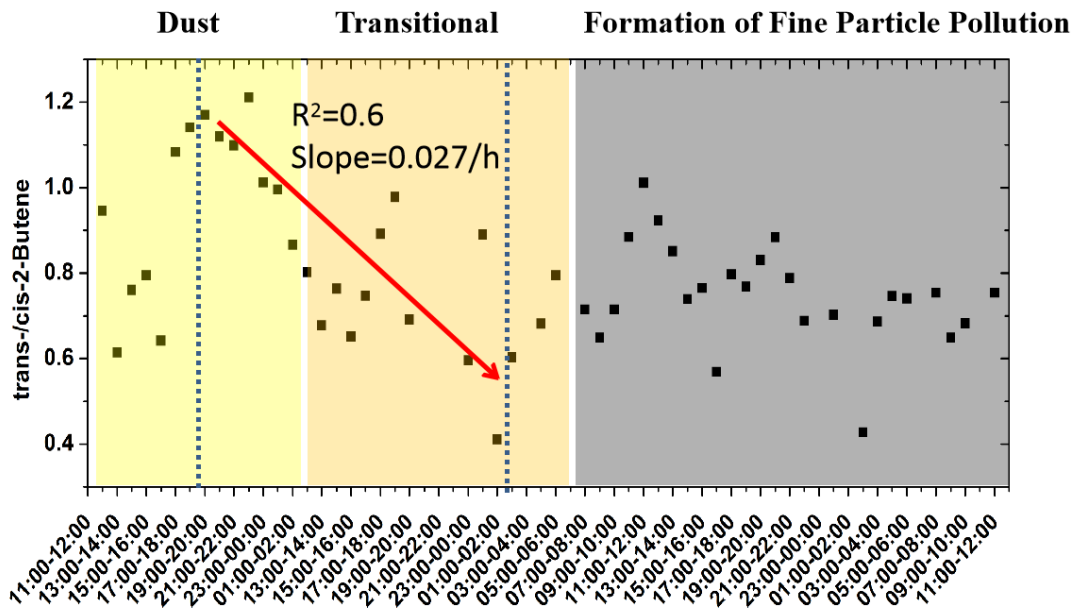
600

601

602

603

604

605

606

607

608

609

610

611



612

613 **Figure 4: Temporal variation of trans-/cis-2-butene ratio in the dust-transitional-fine particle pollution period.**
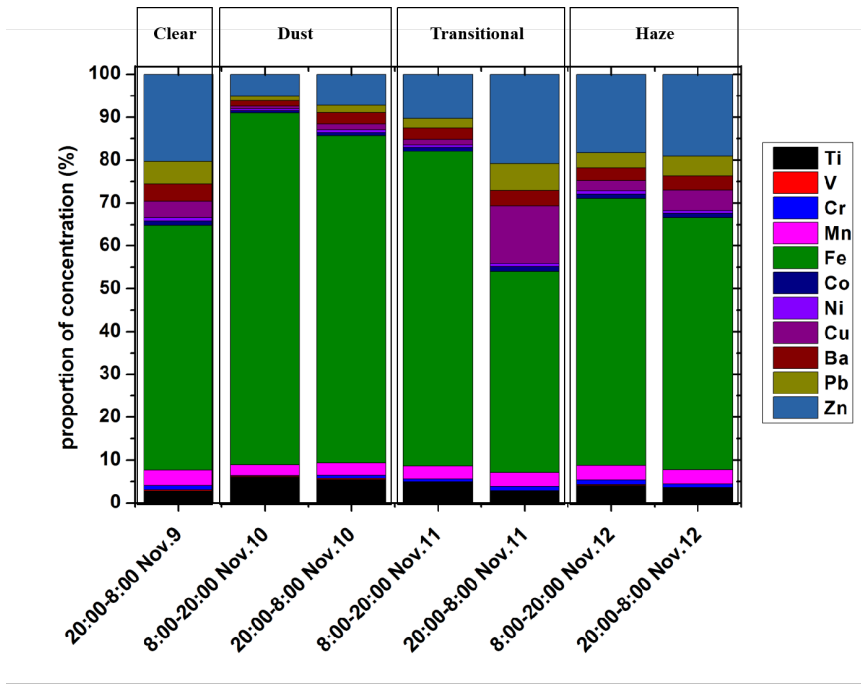
614

615

616

617

618

619

620

621

622

623

624

625

626

627

**Figure 5: Composition of selected metallic elements in the PM2.5 samples.**

628

629

630

631

632

633

634

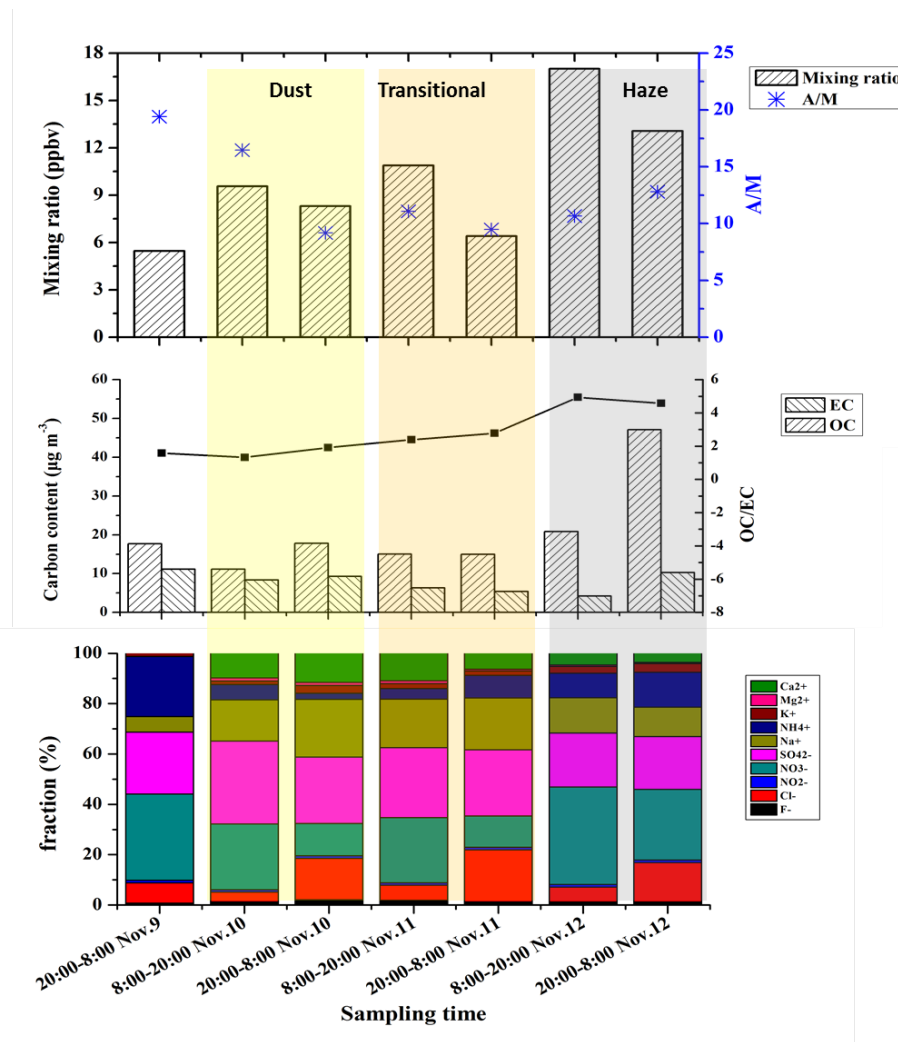635

636

637

638

639

640

641

642

643

644

645

24

646



647

**Figure 6: Variations in (a) the mixing ratios of 17 carbonyl compounds and acetone to methylglyoxal (A/M) ratios in the gas phase, (b) particulate carbon fractions, (c) and particulate water-soluble ions during the study period.**

651

652

653

654

655

656